Complex Nonlinear Behavior in the Full-Scale High-Impact Polystyrene Process

Antonio Flores-Tlacuahuac*

Department of Chemical Engineering, Carnegie-Mellon University, 5000 Forbes Avenue, Pittsburgh 15213, Pennsylvania

Víctor Zavala-Tejeda

Departamento de Ingeniería y Ciencias Químicas, Universidad Iberoamericana, Prolongación Paseo de la Reforma 880, México DF 01210, México

Enrique Saldívar-Guerra

Centro de Investigación en Química Aplicada, Blvd. Enrique Reyna 140, Saltillo, Coahuila CP 25100, México

In this work, the open-loop nonlinear bifurcation analysis of the high-impact polystyrene process is carried out and used for optimal design, operation, and control analysis. The process can be described by a set of seven continuous stirred tank reactors (CSTRs) connected in series. Process design was carried out using an optimization approach; the nominal optimal operating point is open-loop unstable and agrees with typical industrial operating conditions. For the seven CSTRs cascade, as much as 398 steady states were found, but only 11 are considered as industrially feasible; 9 of them are open-loop unstable. Both input and output multiplicities were found, and implications on optimal grade transitions and process control are discussed. A simple cascade control system was used to demonstrate that linear PI controllers add patterns of nonlinear behavior previously not present in the process.

1. Introduction

Polymer manufacture involves processes that can exhibit highly nonlinear behavior including phenomena such as input/output multiplicities, limit cycles, sustained oscillations, hysteresis, chaos, etc.[1] Nonlinear analysis tools are useful to locate the range of design parameters over which complex operating regimes may occur.[2] They also permit one, for instance, to set up control schemes able to address issues embedded by intrinsic nonlinear behavior.[3] Since process plants are now required to be more flexible, a consideration of nonlinearities is necessary to have confidence in model predictions concerning plant operation over a wide range of operating conditions. Commonly, nonlinearities are perceived as an undesired phenomenon because they may adversely affect product quality and process control and lead to unsafe operations.[3] It is widely accepted that processes must be designed and operated not only to optimize static performance but also to impart the system with accepted levels of controllability and resiliency.[4] Thus, nonlinear analysis is potentially helpful in early design stages. Initial efforts to take into account nonlinear behavior in an optimization design framework have been recently reported.[5] Even when nonlinearities are commonly considered harmful to process operation, there might be cases when optimal static design calls for operation around highly nonlinear regions. It is a common rationale that, although feasible operation of open-loop unstable systems is possible by adequate feedback control, such a situation is usually undesirable because of operability and safety reasons and should be avoided by proper design. Some authors have proposed design procedures for stable operations in a single continuous stirred tank reactor (CSTR).[6] Kokossis and Floudas[7] formulated an optimization approach with open-loop stability constraints (i.e., trough the eigenvalues of the mathematical model Jacobian matrix) to achieve stable optimal solution for the synthesis of complex reactor networks. Nevertheless, there are evidences of complex processes in which stable operating points might not be profitable. Blanco et al.[8] developed an optimal redesign of the Tennessee Eastman Challenge Process (TECP), which features an open-loop unstable recycle reactor capable of reaching shutdown limits in a few hours even for small disturbances. The purpose of their work was to find an open-loop stable optimal operating point formulating an eigenvalue optimization problem. Although a feasible stable steady state was found, the redesigned optimal conditions increased process operating costs about 20 times with respect to the unstable nominal operating point. Examples such as this one should lead us to question whether it is time not to overlook nonlinearities and to take advantage of their intrinsic presence.[2]

Complicated nonlinear bifurcation behavior has been reported in several types of single polymerization reactors, this phenomena can be predicted from process models, demonstrated in laboratory reactors, and experienced in a wide range of industrial processes.[1] Complex kinetic behavior, mass- and heat-transfer limitations, and the presence of the gel effect are some identified sources of complex bifurcation behavior in polymerization reactors.[9] Nonlinear behavior of single continuous stirred tank reactors has been widely studied. Some pioneer work was developed by Van Heer-

* To whom correspondence should be addressed. On leave from Universidad Iberoamericana. E-mail addresses: antonio.flores@uia.mx; aflores2@andrew.cmu.edu. Phone/fax: +52(55)59504074. URL: http://200.13.98.241/~antonio.

10.1021/ie049418m CCC: $30.25
Published on Web 02/18/2005

den[10] and Aris and Amundson,[11] while the complete treatment of nonlinearity and bifurcation of a CSTR with a single reaction was addressed by Uppal et al.[12] Advances obtained from these early works motivated studies in more complex reaction kinetics, such as those found in polymerization reactors. Ray and Villa[1] have recently reviewed nonlinearity issues commonly embedded in polymerization reaction systems. In the case of multiunit polymerization processes, they might display complex nonlinear behavior since its dynamic behavior depends not only on the characteristics of the individual units but also on the topology of the flow sheet.[13]

Owing to both theoretical and numerical complexities when dealing with sequences of connected reactors, few works have been reported on the bifurcation behavior of more than two coupled reactors. Dangelmayr and Stewart[14] analyzed the *N*-CSTRs cascade as a sequential bifurcation problem. A systematic work on the multiplicity and stability problem of two coupled nonisothermal CSTRs was developed by Kubicek et al.,[15] who studied the effect of the recirculation ratio on the stability and concluded that multiplicity of the system is decreased as the recycle rate increases. Varma[16] set up a conservative upper bound of steady-state solutions for a sequence of *N* CSTRs connected in series. He concluded that a large number of steady states may emerge even for a few-tank sequence and that a small number of these steady states are stable. Snovoros et al.[17] studied the steady-state multiplicity and stability of two identical coupled CSTRs. They found that up to seven steady states can arise for a given Damköhler number, but only three of these are stable, in agreement with the Varma and Kubicek results. To our best knowledge, even for simple reactions, no works have been reported on the complex nonlinear behavior of coupled reactors.

In this work, we perform a full-scale steady-state nonlinear bifurcation analysis of the reaction train of a typical high-impact polystyrene (HIPS) process. HIPS is one of the most important synthetic polymers. It is normally manufactured by the bulk polymerization of styrene in the presence of small amounts of polybutadiene, which is added to promote better mechanical properties.[18] Polymerization can be thermally or chemically initiated with monofunctional and bifunctional initiators. There are several variations of the production process, but as displayed in Figure 1a, most of them employ a continuous stirred tank reactor (CSTR) in series with some kind of tubular reactor(s). Commonly, a heat exchanger is employed at the end of the reaction train to convert the remaining monomer. In this work, the tubular reactors have been approximated by a set of five series-connected CSTRs, while the heat exchanger performance has been approximated by a single CSTR. Therefore, as shown in Figure 1b, the complete HIPS polymerization reaction train is composed of a set of seven series-connected CSTRs featuring no recycling streams among them. Because of the complexity of the HIPS reaction train mathematical model, which features about 120 ordinary differential equations and a complex kinetic mechanism, a purely numerical continuation procedure is employed as a way to characterize the HIPS process nonlinear steady-state behavior.

The aim of this work is to provide a comprehensive nonlinear bifurcation analysis and implications on process design, operation, and control of the reaction train of the HIPS process. Although several works on nonlinear analysis of polymerization reactors are available, there are only a few works on nonlinear analysis of process flow sheets.[13] There are no published works on the nonlinear analysis of the HIPS manufacturing process. In this work, we extend the study conducted by Verazaluce et al.[19] for a single HIPS reactor and analyze the effect of interactions among process units. A simple case of the HIPS process is analyzed, therefore avoiding mathematical modeling complexities. All nonlinear bifurcation diagrams were generated using the MATCONT software.[20]

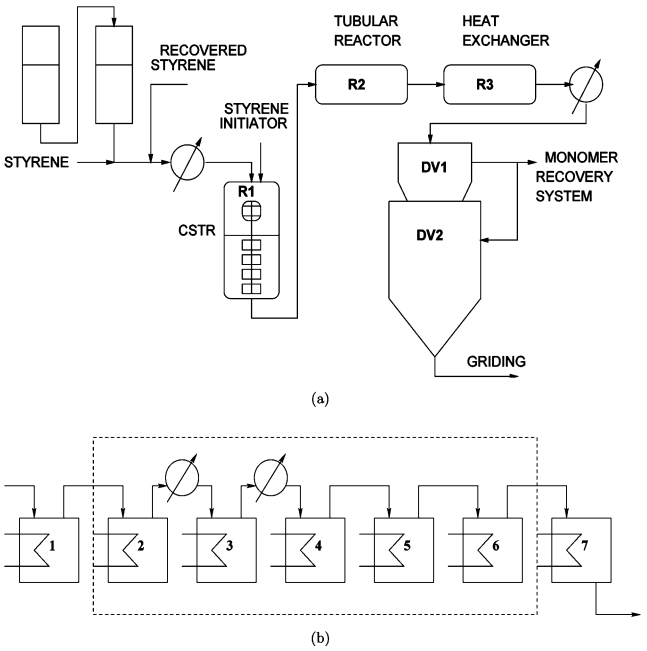

Figure 1. (a) Flowsheet of the HIPS plant and (b) approximation of the HIPS plant by a set of seven series-conneced CSTRs. The dashed box stands for the five CSTRs employed for approximating the steady-state behavior of the R2 tubular reactor.

Optimal design of the process units was carried out to mimic an industrial process performance. Steady-state stability and implications on optimal economic design are discussed. Control limitations and potential closed-loop stabilization are also analyzed. Finally, we use bifurcation maps for setting up start up, shut down, and grade transitions alternatives of the process.

2. Mathematical Modeling

In the open literature, there are only a few works on the modeling of the HIPS process.[21,22] In this part, the mathematical model of the free-radical bulk polymerization of the system styrene/polybutadiene, using a monofunctional initiator, is described. In Figure 1a, a typical industrial process[18] for HIPS manufacturing is shown. The set of polymerization reactions are carried out in a continuous stirred tank reactor followed by a tubular reactor and finally by a heat exchanger. No recycle streams are present in the process. Owing to the complexity of the mathematical model of the tubular reactor, as a first rough approximation, the steady-state behavior of such reactor was approximated by a set of five CSTRs connected in series, thus giving rise to a system of seven series-connected CSTRs as shown in Figure 1b. The steady-state behavior of the reaction train has been matched against experimental plant data. The dynamic behavior of the HIPS process during grade transition has been reported elsewhere;[23] the reaction kinetic mechanism is shown in Table 1. Diffu-

Table 1. HIPS Kinetic Mechanism

Initiation Reactions	
thermal	$3M_S \xrightarrow{k_{i_0}} 2R_S^1$
chemical	$I \xrightarrow{f_i k_d} 2R$
	$R + M_S \xrightarrow{k_{i_1}} R_S^1$
	$R + B_0 \xrightarrow{k_{i_2}} B_R$
	$B_R + M_S \xrightarrow{k_{i_3}} B_{RS}^1$
Propagation Reactions	
	$R_S^j + M_S \xrightarrow{k_p} R_S^{j+1}$
	$B_{RS}^j + M_S \xrightarrow{k_p} B_{RS}^{j+1}$
Definite Termination Reactions	
homopolymer	$R_S^j + R_S^m \xrightarrow{k_t} P^{j+m}$
grafting	$R_S^j + B_R \xrightarrow{k_t} B_P^j$
	$R_S^j + B_{RS}^m \xrightarrow{k_t} B_P^{j+m}$
cross-linking	$B_R + B_R \xrightarrow{k_t} B_{EB}$
	$B_{RS}^j + B_R \xrightarrow{k_t} B_{PB}^j$
	$B_{RS}^j + B_{RS}^m \xrightarrow{k_t} B_{PB}^{j+m}$
Transfer Reactions	
monomer	$R_S^j + M_S \xrightarrow{k_{fs}} P^j + R_S^1$
	$B_{RS}^j + M_S \xrightarrow{k_{fs}} B_P^j + R_S^1$
grafting sites	$R_S^j + B_0 \xrightarrow{k_{fb}} P^j + B_R$
	$B_{RS}^j + B_0 \xrightarrow{k_{fb}} B_P^j + B_R$

sion-controlled effects were considered, and the model used was that proposed by Hui and Hamielec.[24]

In this part, the dynamic mathematical model of the free-radical bulk polymerization of the system styrene/polybutadiene, using a monofunctional initiator, is described. The set of polymerization reactions are carried out in a nonisothermal CSTR assuming perfect mixing, constant physical properties, quasi-steady state, and the long chain hypothesis. Constant volume in the reactor has been also assumed. Changes in density of the monomer−polymer mixture have been neglected. It is assumed that the system is homogeneous. In practice, rubber particles form a separate phase, which is usually small in weight percentage (around 4−6%); therefore, this assumption is a reasonable approximation. The kinetic mechanism involves initiation, propagation, transfer, and termination reactions. Polybutadiene is added to guarantee desired mechanical properties by promoting grafting reactions. Network formation reactions are also modeled because they may lead to an undesirable excess of cross-linking in the rubber particles. There is some debate about the reactions causing cross-linking. It is reasonable to assume that the main reaction responsible for cross-linking occurs between two just activated polybutadiene radicals. However, other authors[25,26] assume that coupling between two radicals in the active ends of graft chains is the main contributor to cross-linking. In this model, both possibilities are included. These modeling considerations have been reported to reproduce the performance of an industrial HIPS continuous stirred tank reactor.[19]

Thereby, using the above modeling assumptions, we describe the mathematical model for each CSTR by the following set of differential equations.

$$\frac{dC_i}{dt} = \frac{F_i C_i^0 - F C_i}{V} - K_d C_i \quad (1)$$

$$\frac{dC_m}{dt} = \frac{F(C_m^0 - C_m)}{V} - K_p C_m(\mu_r^0 + \mu_b^0) \quad (2)$$

$$\frac{dC_b}{dt} = \frac{F(C_b^0 - C_b)}{V} - C_b(K_{i2}C_r + K_{fs}\mu_r^0 + K_{fb}\mu_b^0) \quad (3)$$

$$\frac{dC_r}{dt} = 2f^* K_d C_i - C_r(K_{i1}C_m + K_{i2}C_b) \quad (4)$$

$$\frac{dC_{b_{eb}}}{dt} = \left(\frac{K_t}{2}C_{b_r}\right) - \frac{F}{V}C_{b_{eb}} \quad (5)$$

$$\frac{dC_{b_r}}{dt} = C_b(K_{i2}C_r + K_{fb}(\mu_r^0 + \mu_b^0)) - C_{b_r}(K_{i3}C_m + K_t(\mu_r^0 + \mu_b^0 + C_{b_r})) \quad (6)$$

$$\frac{d\mu_r^0}{dt} = 2K_{i0}C_m{}^3 + K_{i1}C_rC_m + C_mK_{fs}(\mu_r^0 + \mu_b^0) \quad (7)$$

$$\frac{d\mu_r^1}{dt} = (R_2\mu_r^1 + R_3(\mu_r^1 + \mu_r^0)) - \frac{F}{V}\mu_r^1 - (K_pC_m + K_t(\mu_r^0 + \mu_b^0 + C_{b_r}) + K_{fs}C_m + K_{fb}C_b)\mu_r^0 + K_pC_m\mu_r^0 \quad (8)$$

$$\frac{d\mu_b^0}{dt} = K_{i3}C_{b_r}C_m - (K_pC_m + K_t(\mu_r^0 + \mu_b^0 + C_{b_r}) + K_{fs}C_m + K_{fb}C_b)\mu_b^0 + K_pC_m\mu_b^0 \quad (9)$$

$$\frac{d\mu_b^1}{dt} = (B_1 + B_2\mu_b^1 + B_3(\mu_b^1 + \mu_b^0)) - \frac{F}{V}\mu_b^1 \quad (10)$$

$$\frac{d\lambda_p^0}{dt} = \left(\frac{K_t}{2}(\mu_r^0)^2 + (K_{fs}C_m + K_{fb}C_b)\mu_r^0\right) - \frac{F}{V}\lambda_p^0 \quad (11)$$

$$\frac{d\lambda_p^1}{dt} = (K_t\mu_r^1\mu_r^0 + (K_{fs}C_m + K_{fb}C_b)\mu_r^1) - \frac{F}{V}\lambda_p^1 \quad (12)$$

$$\frac{d\lambda_{b_p}^0}{dt} = (K_t\mu_r^0(\mu_b^0 + C_{b_r}) + (K_{fs}C_m + K_{fb}C_b)\mu_b^0) - \frac{F}{V}\lambda_{b_p}^0 \quad (13)$$

$$\frac{d\lambda_{b_p}^1}{dt} = (K_t(\mu_r^1C_{b_r} + (\mu_r^1\mu_b^0 + \mu_r^0\mu_b^1)) + (K_{fs}C_m + K_{fb}C_b)\mu_b^1) - \frac{F}{V}\lambda_{b_p}^1 \quad (14)$$

$$\frac{d\lambda_{b_{bp}}^0}{dt} = \left(K_t\mu_b^0C_{b_r} + \frac{K_t}{2}(\mu_b^0)^2\right) - \frac{F}{V}\lambda_{b_{bp}}^0 \quad (15)$$

$$\frac{d\lambda_{b_{bp}}^1}{dt} = (K_t\mu_b^1C_{b_r} + K_t\mu_b^1\mu_b^0) - \frac{F}{V}\lambda_{b_{bp}}^1 \quad (16)$$

$$\frac{dT}{dt} = \frac{F(T^0 - T)}{V} - \frac{\Delta HK_pC_m(\mu_r^0 + \mu_b^0)}{\rho_sC_{ps}} - \frac{UA(T - T_j)}{\rho_sC_{ps}V} \quad (17)$$

$$\frac{dT_j}{dt} = \frac{F_j(T_j^0 - T_j)}{V_j} + \frac{UA(T - T_j)}{\rho_jC_{pj}V_j} \quad (18)$$

here

$$R_1 = 2K_{i_0}C_m^{\ 3} + K_{i_1}RC_m + K_{fs}\mu_b^0 \quad (19)$$

$$R_2 = -(K_pC_m + K_t(\mu_r^0 + \mu_b^0 + C_{b_r}) + K_{fb}C_b) \quad (20)$$

$$R_3 = K_pC_m \quad (21)$$

$$B_1 = K_{i_3}C_{b_r}C_m \quad (22)$$

$$B_2 = -(K_pC_m + K_t(\mu_r^0 + \mu_b^0 + C_{b_r}) + K_{fs}C_m + K_{fb}C_b) \quad (23)$$

$$B_3 = K_pC_m \quad (24)$$

The number average chain length is given by

$$M_n = M_w\left(\frac{\lambda_p^1 + \mu_r^1}{\lambda_p^0 + \mu_r^0}\right) \quad (25)$$

where C stands for concentration, T is the reactor temperature, the subscripts i, m, b, and r stand for initiator, monomer, butadiene, and radical, respectively, and the subscripts o and j mean feed stream and jacket-related variables, respectively. μ^0 is the zeroth moment of the death species, F is the feed stream volumetric flow rate, V is the volume, f^* is the initiator efficiency, ΔH is the reaction heat, ρ is the density, and C_p is the heat capacity. K stands for the kinetic rate constants and its subindexes d, p, i_0, i_1, i_2, i_3, k_t, k_{fs}, k_{fb} represent the rate constants of the different polymerization steps. Finally, M_w stands for the styrene molecular weight. The details of the kinetic mechanism, rate constants, and design parameters are contained in ref 19.

3. Optimal Process Design

Optimal design of the seven series-connected CSTRs cascade was sought in such a way that actual industrial monomer conversion ranges were matched. In a typical industrial process,[23] a feed stream consisting of styrene monomer, polybutadiene, and initiator is fed to the reactor train (see Figure 1a). The first reactor (R1) is operated at around 120−130 °C and a conversion of 20−30% is achieved there. The product stream is sent to a second reactor (R2) which, in the particular process analyzed here, is an isobaric tubular reactor operating at around 160−170 °C where a 60% global conversion is normally achieved. Next, the product stream from R2 is fed to a heat exchanger operating at around 200 °C where the polymerization reaches around 70% global conversion. As it was mentioned before, the complete HIPS reaction train was approximated by a set of seven series-connected nonisothermal CSTRs as shown in Figure 1b. In this figure, the dashed box represents the five CSTRs employed to approximate the tubular reactor behavior. Our industrial experience with the HIPS process suggests that five CTRS suffices to approximate the tubular reactor steady-state behavior;[23] such number of reactors was determined by inserting the right number of CSTRs until plant data was approximately matched.

The optimization problem decision variables considered are typical reactor design parameters such as volume, jacket dimension, heat transfer area, and cooling water flow rate, which lead to a suitable conversion profile such as the one described above. Therefore, for each reactor, the design of each CSTR was cast in terms of the following NLP.

$$\min_{\mathbf{x},\mathbf{u}} (X_i^d - X_i)^2$$
$$\text{s.t.}$$
$$\text{eq 1} - \text{eq 9} = 0$$
$$0 \le \theta_i \le \theta_i^u$$
$$293 \le T_i^{\text{jacket}} \le 373 \text{ K}$$
$$\mathbf{x}, \mathbf{u} \ge 0 \qquad \forall\{i \in 1, ..., 7\} \quad (26)$$

where i stands for the reactor number in the cascade, $\mathbf{u}$ is the set of design parameters $[V, V_j, A, Q_{cw}]$ for every reactor i, and $\mathbf{x}$ are the system states. θ (h) is the residence time, and $\theta^u = [1.5, 0.1, 0.1, 0.1, 0.1, 0.1, 1.2]$ is the residence time (h) upper bound. $X_i^d = [0.15, 0.35, 0.5, 0.60, 0.7, 0.7, 0.75]$ is the desired global conversion reached in each reactor, and X_i is the actual optimum global fraction conversion in the same reactor. Global here means that the monomer conversion is calculated from the feed stream to the sequence up to the ith reactor outlet.

Table 2. Optimal Values of the Decision Variables

reactor	vol (L)	jacket vol (L)	Q_{cw} (L/s)	heat-transfer area (m²)
1	6000	1200	0.1311	11.718
2	900	180	1.0	1.7578
3	1000	200	1.0	1.9531
4	650	130	1.0	1.2695
5	1000	200	1.0	1.9531
6	1000	200	1.0	1.9531
7	5000	1000	1.0	9.5676

Table 3. Nominal Steady State of the HIPS Reaction Train

reactor	C_m (mol/L)	T_r (K)	T_j (K)	T_o (K)
1	7.318	377.460	347.304	333.000
2	5.388	454.356	299.387	377.460
3	3.860	464.848	300.353	408.920
4	3.578	445.925	297.720	441.605
5	3.375	434.152	299.212	437.006
6	3.240	428.635	299.006	434.132
7	3.158	394.283	310.231	428.635

Optimal design information is presented in Table 2, while nominal steady-state conditions for the process are presented in Table 3. The optimization problem was solved using the mathematical modeling software AMPL[27] and IPOPT[28] for solving the NLP problem. Under the optimization framework proposed, it was found that conversion levels in the tubular reactor (reactors 2−6) were extremely sensitive to small variations in the operating temperature. This phenomenon is influenced by the gel effect onset. Under this situation, the viscosity of the polymeric mixture tends to rise sharply, therefore leading to a decrease in mass diffusion. Because of this, the released heat of reaction cannot be efficiently removed, giving rise to large temperature increases. In fact, the onset of the gel effect has been recognized as a major nonlinearity source in polymerization systems. It was found that employing reactor intercooling might permit one to overcome thermal runaway conditions, making it feasible to operate the process around the industrial desired monomer conversion range. Analyzing the conversion profile for the process, see Figure 5,

Table 4. Process Total Steady-State Solutions

CSTR no.	total	unstable	stable
1	3	1	2
2	7	4	3
3	14	10	4
4	26	21	5
5	49	43	6
6	83	76	7
7	216	208	8
Σ	398	363	35

one can notice that most of the polymer chains are produced in reactors 1−3 (55%), while in the final reactors 4−7, only an additional 8% is reached. This was only possible when intercooling stages were set between reactors 2 and 3 and 3 and 4 leading to a fixed cooling capacity of 20 °C. Using this design modification, we achieved an additional 10% conversion increase. Actually, some polymerization tubular reactors are designed to allow reaction mixture intercooling to avoid gel effect limitation on monomer conversion. Once the desired conversion level in the tubular reactor is achieved, the common industrial practice is to send this product stream into a final heat exchanger aimed to consume an additional amount of styrene. However, because the rate of reaction in the heat exchanger tends to be low, leading to small amounts of released heat, the feed stream might require extra heating, though in this work no preheating was employed. Therefore, the final global conversion obtained is around 65%. This optimal design will be taken as the base case for later application of bifurcation analysis.

The optimal nominal operating point is open-loop unstable. For this particular process, there are no open-loop stable steady-state design conditions that can yield the desired conversion levels. Although, the steady-state optimization approach has been widely used for systematic design of chemical processes, key parameters are often constrained to keep the processes away from operating near or within regimes characterized by steady-state multiplicity or sustained periodic oscillations among other nonlinear phenomena. This situation may prevent design and operation near more profitable steady-state economic optima.[2] Such nonlinear operating regimes can be a desired alternative from the economic point of view. Furthermore, with new nonlinear programming strategies being developed to permit reliable and robust model predictive control (MPC) near or within complex nonlinear operating regimes,[29] the instability open-loop problem might be an issue not hard to deal with. For instance, Prasad et al.[30] have applied MPC techniques to a jacketed styrene polymerization reactor using multirate and state estimation techniques.

4. Steady-State Multiplicity and Stability

Before nonlinearity maps were computed, an effort was made to get an idea about the number of expected steady-state solutions. Varma[16] set up a conservative upper bound of steady-state solutions for a cascade of N CSTRs in which a single A → B exothermic reaction was carried out under isothermal conditions. He concluded that such a sequence can have up to $2^{N+1} - 1$ steady states of which only $N + 1$ are stable. This means that a sequence of seven CSTRs might feature 255 steady-state solutions, but only 8 steady-state solutions might be stable. Morever, Varma's results were obtained for a simple kinetic system. Thereby, for more complex

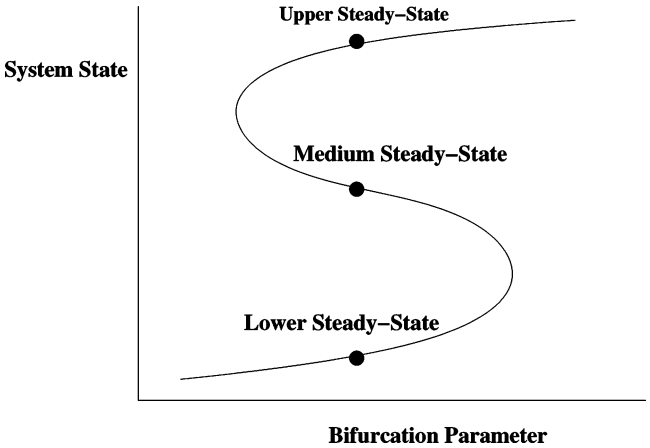

Figure 2. Classical three-state multiplicity behavior.

kinetic systems, the number and stability of steady states may vary depending on the kinetic mechanism and physical limitations. According to Varma's prediction, a large number of steady-state solutions should be expected for the system of seven series-connected CSTRs. This was indeed the case. For instance, 216 steady-state solutions were found at the seventh reactor in the cascade, but only 11 of these are considered as industrially feasible. Of these, 9 steady states turned out to be open-loop unstable, and they were located around the desired operating region, remarking the need to operate the process around unstable steady states to achieve attractive conversion levels. For each reactor, the total number of steady states and their stability characteristics are shown in Table 4. As shown in this table, only around 10% of the steady states turned out to be open-loop stable. As seen, Varma's upper bound underestimates the number of steady states by 56%. Anyway, owing to the complex dynamic behavior, one should probably consider Varma's result as a conservative upper bound. All the steady states were found using standard continuation techniques embedded in MATCONT.[20]

Another implication of Varma's results relies on the proportion of unstable over stable steady-state solutions, which might lead us to conclude that even in CSTR sequences with simple kinetics, the possibility of stable operation is low. As a result, operation around unstable regions should not be avoided based only on operability grounds; sometimes open-loop unstable steady states might be one of the best ways to run a process. In particular, this is especially true in polymerization reactors, which display the classic three steady-state pattern (see Figure 2). Here the intermediate steady state is always unstable, while the upper and lower steady states might be either stable or unstable. Operation at the lower steady state is not profitable owing to low conversion yields. From an economic point of view, the upper steady state would be preferred if not for the presence of the gel effect. Hence, the intermediate steady state, which features open-loop instability, is better suited to carry out the polymerization reactions; yield is not as high, but the onset of the gel effect is avoided.

One might consider that the approximation of the tubular reactor by a series of five series-connected CSTRs could introduce spurious steady states. It is worth remarking that the steady-state multiplicity pattern of the five series-connected CSTR approximation of the tubular reactor is not necessarily in conflict with

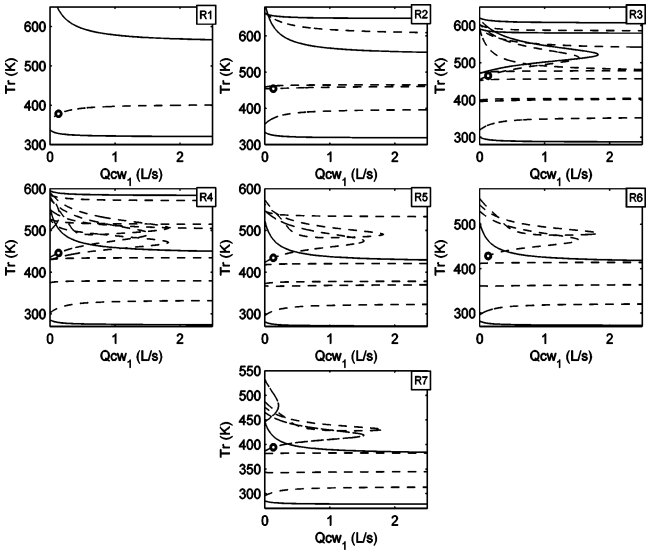

Figure 3. Steady-state solutions explosion for the series-connected CSTR cascade.

the nonlinear behavior of tubular reactors. There are some evidences of complex steady-state multiplicity behavior found in tubular reactors even for simple kinetic mechanisms.[31]

To set a clear idea about the explosion in the number of steady states as reactors are added to the sequence of CSTRs, let us consider Figure 3, which displays bifurcation diagrams for all seven series-connected CSTRs, using the cooling water flow rate of the first reactor as the continuation parameter. As usual, open-loop stable steady states are denoted by the continuous line, while open-loop unstable steady states are denoted by dashed lines. The symbol "o" stands for nominal operating conditons. As commonly occurs, under nominal operating conditions, the first reactor only exhibits three steady states. According to the aforementioned discussion, only the intermediate unstable operating point is feasible, since it operates far from the gel effect onset. The nonlinearity map starts becoming complicated moving downstream and adding a second reactor. The second reactor exhibits up to seven steady states. Of the seven steady states, only three are stable and four are unstable. The high conversion steady state of the first reactor only "generates" one steady state in the second reactor, each one of the medium and low temperature steady states generated up to three solutions. When one moves beyond the third reactor, the number of steady states increases even more. For simplicity, only the steady states around the feasible operating point are shown. The same pattern regarding the increase of steady-state solutions occurs when the 4−7 CSTRs are added. It should be highlighted that in all the reactors, the nominal operating point is always unstable. In interlinked systems,[32] the emergence of additional multiple steady states has been attributed to the connections among processing equipment, which might be the situation for processes featuring recycling or feedback streams, though in our case no recycling streams are present. Thereby, high nonlinearities are possibly the only form to explain the explosion in the number of steady-state operating points. It is worth noting that the infeasibility regions shown in Figure 3 (reactor 1) are similar to those reported by other authors.[33]

5. Process Bifurcation Analysis

Numerical continuation techniques are employed to trace all the bifurcation diagrams. Due to the number of CSTRs analyzed and the complex kinetic mechanism involved, the resulting system of ordinary differential equations to be solved is precisely 133. Only steady-state branches of solutions are presented here, since the problem of finding branches of periodic solutions relies on the solution of a much higher-dimensional system of equations.[34] The analyzed sequence of cascade reactors presents an extremely large number of steady-state solutions as discussed before. Therefore, the bifurcation analysis will be focused in a small space of solutions around the nominal operating point.

In Figure 4, bifurcation diagrams of the temperature, global conversion, number-average molecular weight, and jacket temperature of the process reactor outlet (R7) using process feed stream temperature as the main continuation parameter and feed stream volumetric flow rate as the secondary parameter are shown. The solution branches represent operating regimes around nominal operating conditions; there process operation might be profitable. The system, as expected, exhibits input and output multiplicities. It can be noticed that all solution branches are unstable. This implies that the process can reach shutdown limits in the presence of even small disturbances of process feed stream in a few hours or even minutes without proper feedback control. Only closed-loop operation of the process is possible, and avoidance of input multiplicities may be achieved by imposing constraints to the process manipulated variables.

The existence of output multiplicities has an adverse effect on feedback control performance. Output multiplicities are characterized by ignition/extinction behavior (limit point instabilities) in which the system becomes open-loop unstable. In R7, this is not the case since there are no stability changes along the solution branches. R7 output multiplicities cannot be removed by manipulating the process feed stream flow rate. Input multiplicities might lead to a harder control problem and can complicate optimal design analysis since the same conversion, molecular weight, and reactor temperature solutions might be achieved for a given continuation parameter.

In Figure 5, bifurcation diagrams of reactors R1 (initial reactor), R2 and R3 (representing the initial tubular reactor length), and R7 (heat exchanger) using process feed stream volumetric flow rate as the main continuation parameter are presented. The nominal operating point is denoted by number 1 and number 2 is another hypothetical operating point. At R1, a styrene conversion of about 15% is achieved under nominal operating conditions. A higher styrene conversion in the reactor can be reached by increasing the process feed stream flow rate. However, in R2, the reactor behavior is quite different. If the process is moved from point 1 to point 2, a small decrease in the styrene conversion will occur. In R3, the nominal solution branch B1 is compacted at around 60% of global conversion. No value of the feed stream flow rate leads to a higher conversion region, even though these conversions are close to those of the gel effect onset. This effect manifests itself in the reactors downstream the process, as can be observed in Figure 5 in the plot corresponding to reactor 7. This behavior should be contrasted against reactor 7 outlet. Here, similar changes in the monomer flow rate give

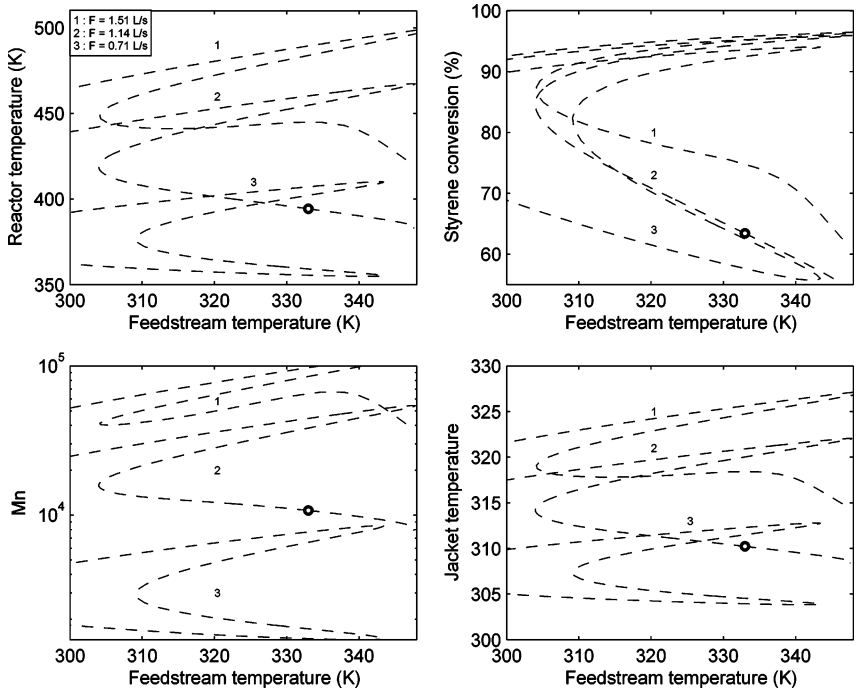

Figure 4. R7 continuation diagrams using the feed stream temperature and volumetric feed stream flow rate as continuation parameters.

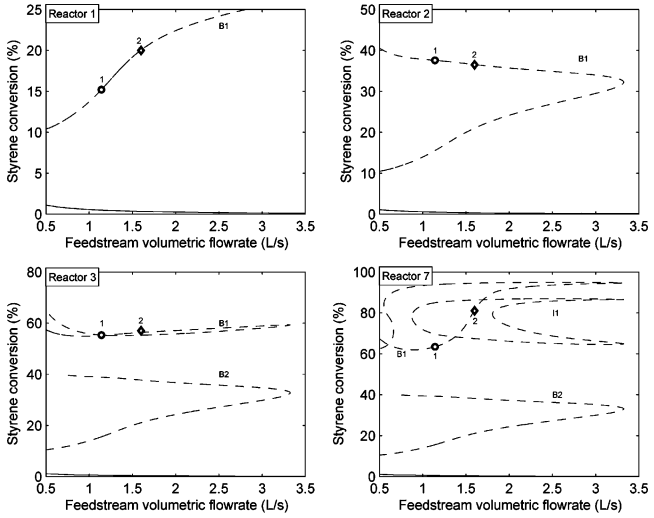

Figure 5. R1, R2, R3, and R7 continuation diagrams using the volumetric feed stream flow rate as continuation parameter.

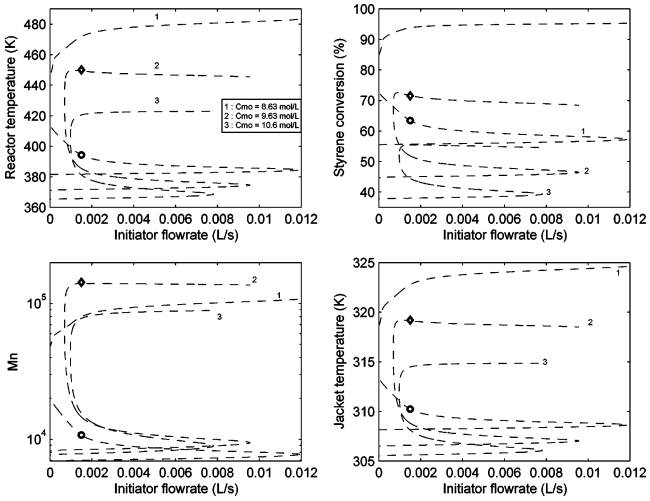

Figure 6. R7 continuation diagrams using the initiator flow rate and monomer feed stream concentration as continuation parameters.

rise to a large conversion degree. Globally speaking, this is a clear manifestation of the intrinsic and highly nonlinear behavior embedded in the model process. This is expected since most of the polymer chains are produced in reactors R1, R2, and R3. In R3, the reactor has reached a temperature of about 180 °C. A common practice in polymerization tubular reactors is the partial cooling of the reaction mixture. So, a part of the reaction mixture is withdrawn, cooled, and returned to the tubular reactor. The aim of the intercooling is to control the temperature within the reactor, avoiding a thermal runaway and the corresponding loss of control. An insight of the nonlinear complexity of the process is evident from Figure 5. Here, the appearance of branch solutions is clear from one reactor to another. This phenomenon is interesting since complex nonlinear regimes can be found without the presence of backmixing in the process (i.e., no recirculation streams). Isola behavior is evident in this bifurcation diagram; the B1 branch is an example of this behavior. Branch B2 generates isolas in R4, R5, and R6 and is extended through R7, and it is denoted by I1. Bifurcation diagrams for R4, R5, and R6 have been omitted since their behavior is not important for discussion purposes.

In Figure 6, bifurcation diagrams for R7 using the process initiator flow rate are presented. All solution branches are unstable. Again, output multiplicities are observed. This means that for a given initiator flow rate, several conversion levels can be achieved. An interesting implication of this behavior can be observed from branches 1 and 2 (at constant initiator flow rate of 1.5×10^{-3} L/s). The high conversion region can be displaced from about 90% (branch 1) to 70% (branch 2) by increasing the monomer feed stream concentration from 8.63 mol/L (nominal point ○) up to 9.63 mol/L (point ◇). This situation steers the process to an increase on the polymer molecular weight from 1×10^4 to 2×10^5 giving rise to a different polymer grade. The effect of variations of the initiator flow rate on process final product is an important issue from the design point of

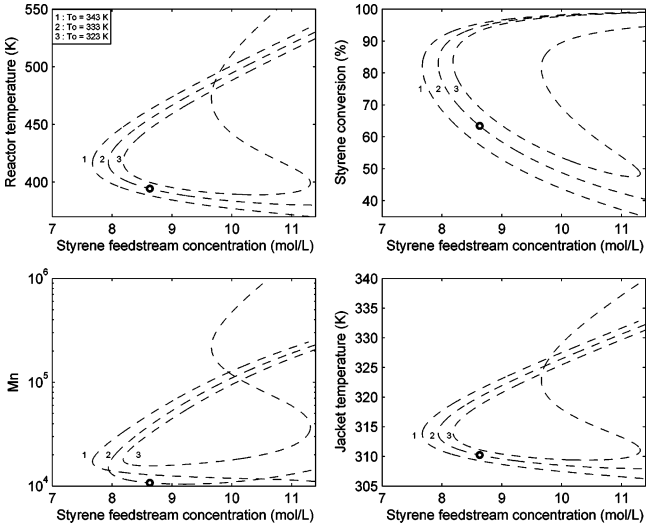

Figure 7. R7 continuation diagrams using the monomer feed stream concentration and feed stream temperature as continuation parameters.

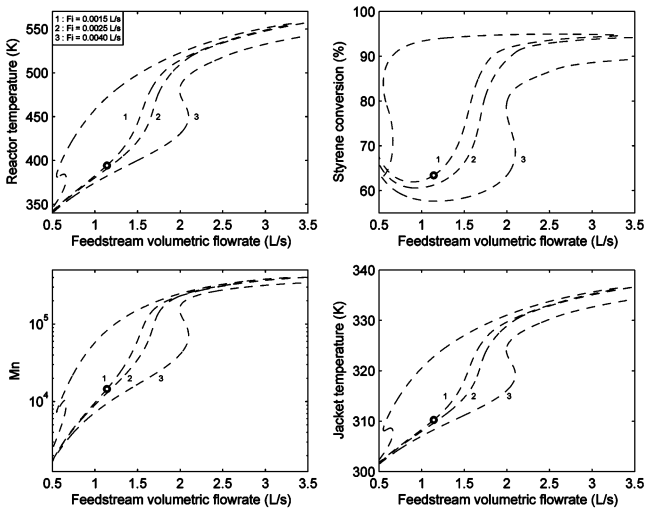

Figure 8. R7 continuation diagrams using the volumetric feed stream flow rate and initiator flow rate as continuation parameters.

view. An optimal process design should minimize initiator consumption, since these reactants are expensive specialty chemicals. From a control point of view, proper initiator flow rate selection can provide controllability and resiliency process characteristics. From Figure 6, it is evident that a small variation in the initiator flow rate might impact severely the process behavior. However, under certain circumstances, this situation may be an attractive feature if the initiator flow rate is employed as manipulated variable for process control purposes.

In Figure 6, the presence of input multiplicities is evident within a small initiator flow rate region. Input multiplicities lead to hard control problems because, under certain conditions, they can be related to inverse response. The connection between input multiplicity and inverse response has been proved by Sistu and Bequette.[35] No process variable manipulation can lead to a complete input multiplicity avoidance. Once these kinds of multiplicities are detected, they might be handled by imposing constraints on the manipulated variables that display this kind of behavior. By increasing the initiator flow rate to the process, one can remove input multiplicities and output multiplicities (branch 2) around the nominal operating zone (branch 1). However, if initiator flow rate is further increased, output multiplicities appear again.

In Figure 7, bifurcation diagrams for R7 using monomer feed stream concentration and feed stream temperature as continuation parameters are shown. It should be noticed that the portion of this figure beyond 9.5 mol/L (styrene concentration at 0 °C) is not achievable. Thereby, from this point of view, the figure portion beyond 9.5 mol/L lacks physical meaning. For branches 1 and 2, only output multiplicities are exhibited. If process feed stream temperature is reduced by only 10 K down to 323 K (branch 3), a strange branch appears displaying input and output multiplicities. This kind of nonlinear behavior is sometimes found in polymerization reactors when polydispersity diagrams are analyzed. Abedekun et al.[9] found this kind of behavior in a MMA polymerization CSTR when tracing solution branches for polydispersity as a function of reactor residence time. Another interesting feature of the input multiplicities displayed in Figure 7 is the fact that the input multiplicities appear on all the states.

Complex nonlinear behavior of the process around the nominal operating point is shown in Figure 8. Under nominal operating conditions, the process operates under an isola solution branch (1). Isola emergence and disappearance might be related to process limitations that restrict feasible operation of the process under a proposed set of design and operating conditions. From branch 1, it is evident that feasible operation of the process around nominal conditions is restricted to a zone from 0.5 to 3.5 L/s of feed stream volumetric flow rate. If a higher initiator flow rate is fed to the process, the isola branch disappears leading to a wider operating zone beyond restrictions shown in branch 1. Furthermore, input multiplicities are expected to disappear at higher initiator flow rates, improving process overall controllability characteristics. Another important process behavior feature is observed in this figure. Process throughput might be increased considerably if one moves from nominal operating point to a higher feed stream volumetric flow rate value (2 L/s). Under this operating point, a monomer conversion of around 90% is expected by reducing reactor average residence time. Reactor volumes might be optimized to yield the same conversion level under nominal operating conditions and thus, reduce process overall capital costs. Strong connections between process nonlinearity and optimal design search are expected, and optimal design search becomes a complex issue.

Process feasible region limitations might be additionally analyzed in terms of monomer feed stream concentration as shown in Figure 9. Once again it should be noticed that, as it was stated for Figure 7, the figure portion beyond 9.7 mol/L has no physical meaning. Under nominal operating conditions, process operation is only feasible around a small region of monomer feed stream concentration. Solution branches 1, 2, and 3 are restricted to the zone displayed in these bifurcation diagrams. No feasible operating points are found beyond those limits. Monomer feed stream concentration dominates process behavior, and no evident changes in solution branches are expected if initiator feed stream concentration is altered. From a decrease of monomer feed stream concentration, higher conversion and molecular weights levels are expected, but a process

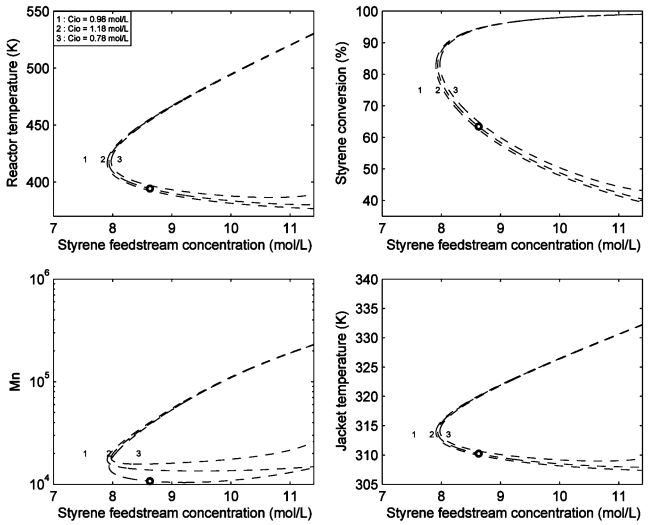

Figure 9. R7 continuation diagrams using the monomer feed stream concentration and initiator feed stream concentration as continuation parameters.

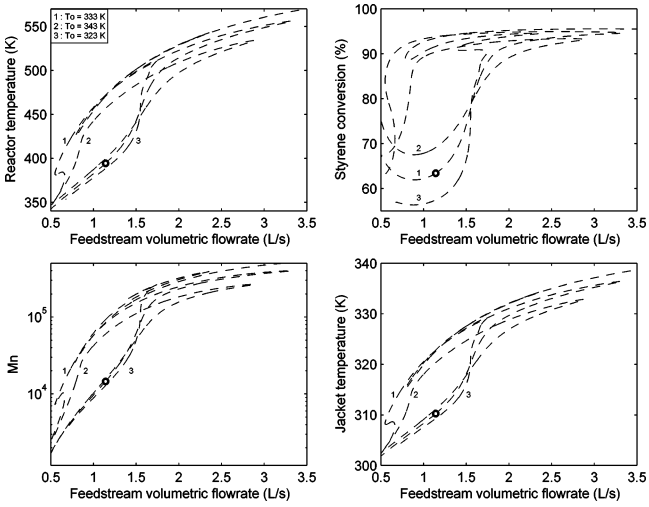

Figure 10. R7 continuation diagrams using the volumetric feed stream flow rate and feed stream temperature as continuation parameters.

capacity decrease is expected as well. Nevertheless, bifurcation diagrams might be useful in early design stages for initial design scenario screening.

In some polymerization processes, feed stream temperature might be used to control exothermicity among reaction units and to avoid input−output multiplicities. This situation is expected to be useful for a single reactor. For series-connected CSTRs, process behavior might not be as predictable as in individual units. This scenario is depicted in Figure 10. Although feed stream temperature is not expected to be changed under normal operation, to change product grade or process throughput, it might be a common operating condition to be analyzed in process design alternatives evaluation. No change in feed stream temperature around realistic bounds will avoid complex nonlinear behavior such as input−output multiplicities. Although, solution branches from reactor temperature and product molecular weight do not vary significantly with changes in feed stream temperature, a change of about 10 °C alters conversion solution branches, and thus, this may be a way to achieve desired grade transitions.

As discussed previously, bifurcation diagrams are important mapping tools in early design alternatives

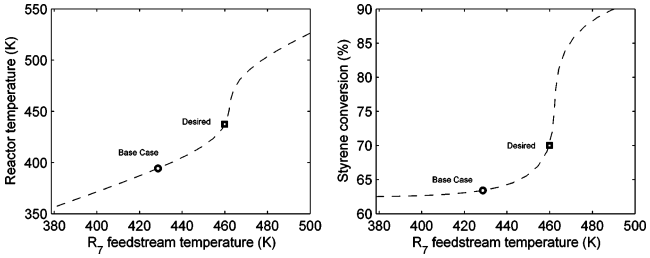

Figure 11. R7 continuation diagrams using R7 feed stream temperature as continuation parameter.

Table 5: Grade Design Information

grade	conversion	T (K)	F_m (L/s)	F_i (L/s)
A	0.635	395	1.14	15×10^{-4}
B	0.83	475	1.62	15×10^{-4}

screening. A simple application of this situation is presented in Figure 11. As discussed in section 3, the common industrial practice in the HIPS process is to terminate the reaction in a heat exchanger. Since the gel effect onset is a conversion limitation, feed stream preheating to the last CSTR will be required to match final conversion levels as exhibited in common industrial practice. A desired final conversion of 70% is expected, but under nominal conditions (with no R7 feed stream preheating), only a 62% of monomer conversion and a stream temperature of about 125 °C are achieved. Figure 11 is used to analyze feed stream heating requirements. An increase of about 50 °C is needed to achieve the required conversion level. A further increase in R7 feed stream temperature might lead to higher conversion levels. This means that final product properties might be also controlled by adjusting only R7 operating conditions (if no important disturbance in previous reaction units is present) despite changing overall process operating conditions, therefore leading to safer operation and reducing product waste possibility.

6. Grade Transitions

Commonly, polymerization plants are run to manufacture different grades of the same kind of polymeric product, operating the process in a multipurpose plant environment. It turns out that end use polymer properties, such as transparency, stiffness, permeability, impact strength, etc., totally depend on the molecular weight distribution and monomer conversion. In turn, those properties are completely determined by the set of operating conditions. In this section, bifurcation diagrams are employed to learn how to pursue efficient grade transition changeover policies.

Let us assume that the so-called A grade corresponds to nominal operating conditions and that plant operating conditions ought to be changed for manufacturing the new desired B grade. As can be noticed from Table 5, the styrene flow rate must be increased by a 50% to produce the B grade leading to a monomer conversion rise from 63.4% up to 87%. Figure 12 displays the bifurcation diagrams between and around the two A and B grades for the complete set of seven series-connected CSTR sequence. Globally speaking, the imposed grade transition change is large, since it implies almost complete monomer conversion. Bifurcation diagrams revel the following useful information: (a) For each grade and in each one of the seven CSTRs, operating conditions give rise to open-loop unstable systems. Thereby, manual grade transition will not be feasible.

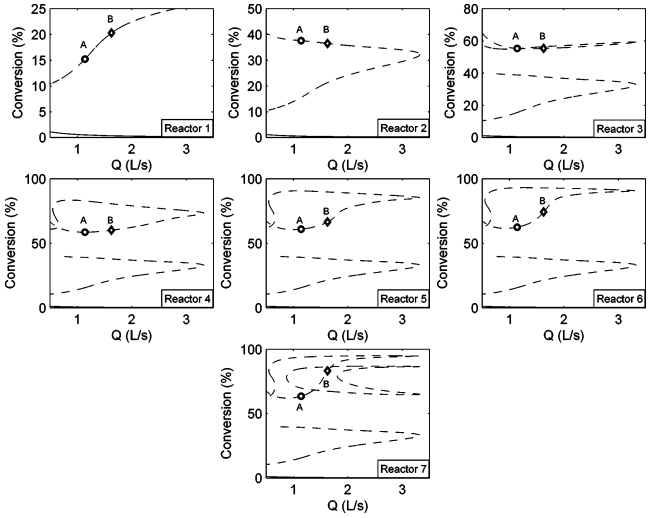

Figure 12. Whole CSTR train continuation diagrams using the volumetric feed stream flow rate as continuation parameter.

Moreover, there are not open-loop stable operating points around the operating regions of both grades. Therefore, instability issues will not be easily removed. (b) The largest monomer conversion variation occurs at the sixth and seventh CSTR, which might be explained on the grounds of the gel effect onset. In contrast, monomer conversion is almost constant at the second, third, and fourth reactors. Actually, monomer conversion tends to decrease at the second reactor, certainly an unexpected scenario. (c) Although the system of seven series-connected CSTRs features a huge number of steady-state solutions, only a small subset of them are feasible, in the sense that such steady-states "window" embeds the operating region of the A and B grades.

Another use of the aforementioned bifurcation maps relates to the computation of the optimal grade transition tracking policy. In fact, bifurcation maps were employed by the authors to select for each one of seven CSTRs process design conditions matching monomer conversion plant data information. Starting with the first reactor, design conditions were sought by solving the nonlinear optimization program discussed in Section 3. Afterward, bifurcation diagrams were obtained to check parametric sensitivity, onset of oscillatory behavior, and operational problems related to the gel effect. The procedure was repeated until all seven CSTRs were designed. Of course, as previously discussed, each time the number of CSTRs was augmented, the complexity and number of steady-state solutions also increased dramatically, specially for the last reactors of the sequence. Following this design procedure, optimal operating conditions for the A grade were determined. Having obtained the bifurcation diagrams of all seven CSTRs of the sequence, it was easier to look for operating conditions for the B grade. Such design grade transition information was used to compute the optimal grade transition policy. The details of the dynamic optimization features will be presented elsewhere.[36] Here, our aim was just to highlight additional issues related to the importance of bifurcation studies when dealing when the process design of highly nonlinear systems.

7. Effect of Feedback Control

Under nominal operating conditions, the steady state of the HIPS reaction train turns out to be open-loop unstable. Therefore, feedback control is required to stabilize the system. Even if the process was open-loop stable, modeling errors and upsets would demand the use of closed-loop control. Although advances in the theory and on-line applications of nonlinear model predictive techniques exist,[29] most chemical processes are still controlled by PID controllers. Commonly, such controllers exploit the natural dynamic behavior embedded in the process, therefore leading to advanced control structures that extend the scope of the traditional feedback loop. Cascade control is one of most widely employed advanced control schemes. It relies on the use of two manipulated variables (as determined by the master and slave control loops) to regulate the value of the controlled variable. Successful performance of cascade control requires that the dynamic behavior of the slave loop ought to be faster than the corresponding one from the master loop.

There are in the literature some works that address the impact of pure feedback PID control on the closed-loop nonlinear behavior,[37−39] while Russo and Bequette[40] have addressed the bifurcation behavior of a cascade-controlled CSTR. It has been reported[39] that even linear plants controlled with a linear controller, subject to input saturation constraints, may lead to complex dynamic behavior. From these studies, it can be concluded that linear PID control tends to introduce nonlinear behavior that was not previously present. One of the worst effects of PID control is the possibility of loosing global stability because of the introduction of additional steady states.[37] Therefore, in this part of the work, an analysis of the potential effects of the cascade control configuration on the closed-loop behavior of the HIPS polymerization system is carried out. For simplicity, only the first CSTR of the reaction train will be examined, but similar or more complex nonlinear patters, will also be present in the rest of the reactors. Therefore, one the aims of the analysis is to highlight the fact that hard nonlinearities will tend to increase in PID closed-loop control systems.

The controlled variable is the reactor temperature. The slave control loop manipulates the cooling water flow rate to control the jacket temperature, while the master control loop sets the set-point of the jacket temperature. Both the slave and master controllers are pure gain proportional controllers. Just for discussion purposes a gain of 30 for the slave controller was selected. In Figure 13, the closed-loop bifurcation diagrams of the cascade control system are displayed. The bifurcation parameter is the gain of the master loop. The hollow circle represents a branching point. Under open-loop conditions, only three steady states were present at the high, medium, and low temperature regions. From Figure 13a, it can be noticed that there is a wide range of master loop gains for which the closed-loop system remains stable. In fact, the closed-loop system loses stability only until the branching point onset. However, in the medium temperature region, no values of the master loop gains are able to closed-loop stabilize the system. It should be recalled that this is the desired operating region. On the other hand, in the low temperature region, the CSTR can be stabilized practically with any master loop gain. However, process operation around this region is infeasible because of the small reaction yield. One of the striking issues of the introduction of the cascade control structure is the loss of global stability properties. From Figure 13b, it can

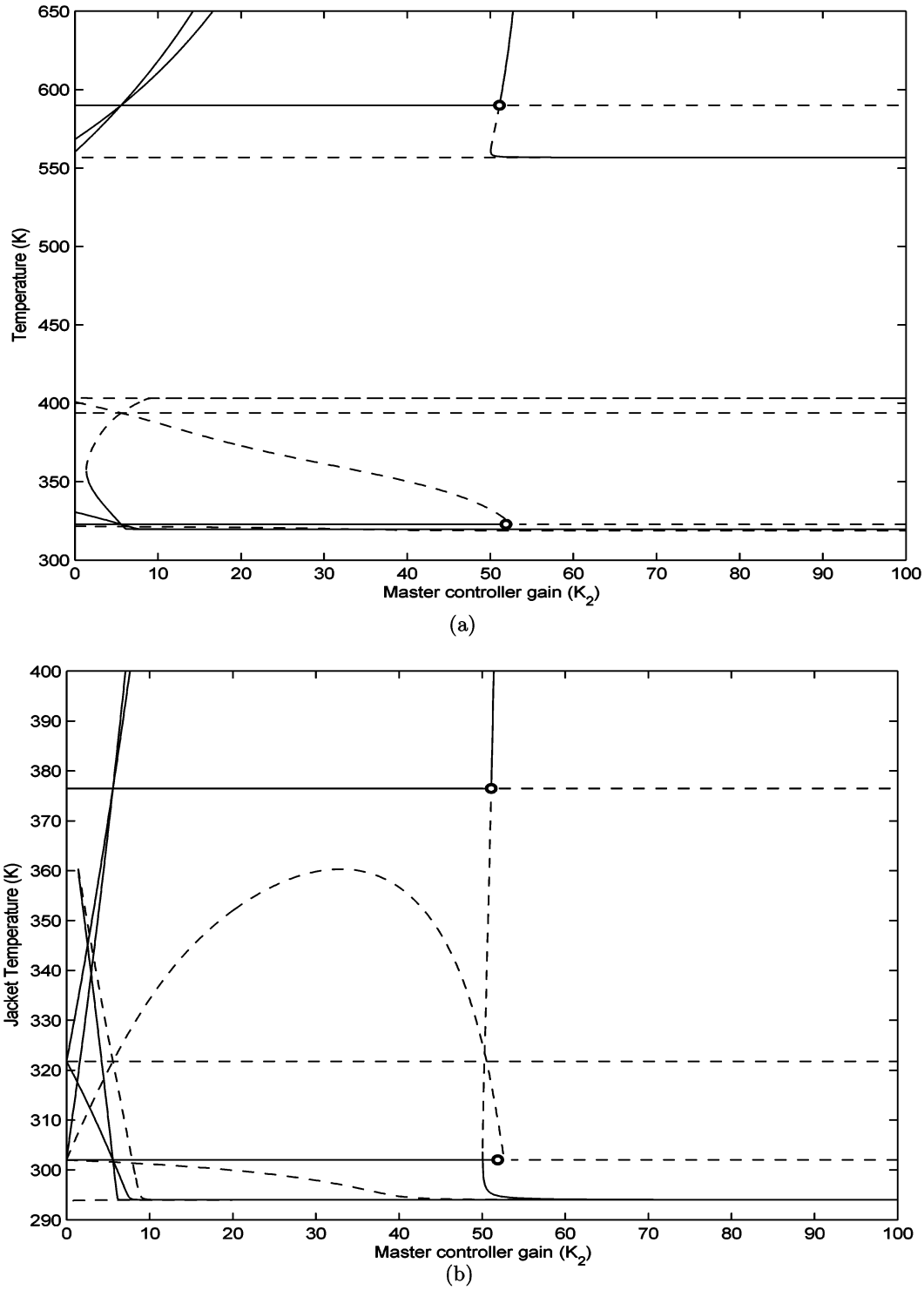

Figure 13. R1 continuation diagrams using the master controller gain as continuation parameter.

be noticed that similar nonlinear patterns can be observed if the closed-loop behavior of the slave loop is analyzed. Globally speaking, the analysis shows that nonlinearities should be taken into account when selecting a control configuration and its tuning parameters. The nonlinear bifurcation analysis might reveal some ways to enhance closed-loop control.

8. Conclusions

In this work, the bifurcation behavior of a complete HIPS plant has been addressed. A mathematical model able to match plant data was used to trace the branches of both open-loop stable and unstable steady states and to locate oscillatory behavior. Complex nonlinearities embedded in the model and the size of the model made necessary the employment of numerical continuation techniques augmented with proper equations to detect singularities. A large number of steady-state solutions were found. The number of steady-state solutions increased moving downstream. Optimal steady-state design of the HIPS process, monomer conversion constraints, and the onset of the gel effect imposed that the operation of the process be located around open-loop unstable regions. Several combinations of potential

manipulated, disturbance, and design variables were examined. For some of these combinations, patterns of multiplicity and oscillatory behavior were observed. A closed-loop cascade controller was used to depict some of the limitations linear controllers impose on the control of highly nonlinear systems. To keep things simple, only the feedback cascade control of the first reactor was addressed. It was found that the cascade controller contributed to increased nonlinearity and destroyed global stability properties.

From the analysis performed, it can be concluded that the closed-loop control of the polyurethane CSTR will impose serious demands on feedback controllers. To achieve satisfactory levels of performance and stability robustness properties, nonlinear control techniques (i.e., MPC) will be required. This is one of the advantages of carrying out bifurcation studies. The use of advanced control techniques might be justified on the grounds of the highly nonlinear patterns that were found. Without undertaking bifurcation studies, it would not be clear whether PID control was enough to keep running the process. It should be stressed that there are few studies addressing the full bifurcation analysis of complete chemical processes.

Nomenclature

A = heat transfer area, m^2
B = grafted polymer, mol/lt
B_o = polybutadiene unit, mol/lt
B_{EB} = cross-linked polybutadiene, mol/lt
B_P = grafted polymer, mol/lt
B_{PB} = cross-linked polymer, mol/lt
B_R = activated polybutadiene unit, mol/lt
B_{RS} = grafted radical with a styrene end group, mol/lt
C_b = polybutadiene concentration, mol/L
C_{b_r} = activated polybutadiene unit, mol/L
C_i = initiator concentration, mol/L
C_m = monomer concentration, mol/L
C_r = radical concentration, mol/L
$C_{b_{eb}}$ = cross-linked polybutadiene, mol/L
C_{ps} = heat capacity, J/(kg K)
F = feed stream volumetric flow rate, L/s
F_i = initiator feed stream flow rate, L/s
I = initiator concentration, mol/lt
K_d = chemical initiation kinetic constant, L/s
K_{fb} = polybutadiene transfer kinetic constant, L/(mol s)
K_{fs} = styrene monomer transfer kinetic constant, L/(mol s)
K_{i_0} = thermal initiation kinetic constant, L/(mol s)
K_{i_1} = chemical initiation kinetic constant (size 1), L/(mol s)
K_{i_2} = polybutadiene activation chemical initiation kinetic constant, L/(mol s)
K_{i_3} = grafted chemical initiation kinetic constant, L(mol s)
K_p = propagation kinetic constant, L/(mol s)
K_t = coupling termination kinetic constant, L/(mol s)
M_s = monomer concentration, mol/lt
M_n = molecular weight distribution
P = homopolymer, mol/lt
T = reactor temperature, K
R = radical concentration, mol/lt
U = global heat-transfer coefficient, J/(s K m^2)
V = volume, L
X_i = monomer conversion in each reactor

Superscripts

0 = zeroth moment
1 = first moment
u = upper bound
d = desired condition

Subscripts

b = grafted polymer
p = homopolymer
j = reactor jacket
o = feed stream condition
i = reactor number

Greek Symbols

ΔH_r = reaction heat, J/mol
λ = moment of a dead species
μ = moment of an active species
ρ = density, kg/L
θ = residence time, s

Literature Cited

(1) Ray, W. H.; Villa, C. Nonlinear dynamics found in polymerization processes—a review. *Chem. Eng. Sci.* **2000**, *55*, 275.

(2) Seider, W.; Brengel, D.; Provost, A.; Widagdo, S. Nonlinear Analysis in Process Design. Why Overdesign To Avoid Complex Nonlinearities? *Ind. Eng. Chem. Res.* **1990**, *29*, 805.

(3) Ray, W. H. Polymerization Reactor Control. *IEEE Control Systems Magazine* **1986**, August, 3−8.

(4) Lewin, D.; Bogle, D. Controllability Analysis of an Industrial Polymerization Reactor. *Comput. Chem. Eng.* **1996**, *20*, S871.

(5) Marquardt, W.; Monnigmann, M. In *Constructive Nonlinear Dynamics in Process System Engineering, Escape-14*; Barbosa, A., Matos, H., Eds.; Elsevier: Amsterdam, 2004; pp 99−116.

(6) Heiszwolf, J.; Fortuin, J. Design Procedure for Stable Operations of First-Order Reaction Systems in a CSTR. *AIChE J.* **1997**, *43* (4), 1060.

(7) Kokossis, A. C.; Floudas, C. A. Stability in Optimal Design: synthesis of Complex Reactor Networks. *AIChE J.* **1994**, *40* (5), 849.

(8) Blanco, A. M.; Bandoni, J. A.; Biegler, L. *Re-design of The Tennessee Eastman Challenge Process: An Eigenvalue Optimization Approach*.

(9) Abedekun, A. K.; Kwalik, K. M.; Schork, F. J. Steady-State Multiplicity During Solution Polymerization of Methyl Methacrylate in a CSTR. *Chem. Eng. Sci.* **1989**, *44*, 2269.

(10) Van Heerden, C. Autothermic Processes: Properties and Reactor Design. *Ind. Eng. Chem.* **1953**, *45*, 1242.

(11) Aris, R.; Amundson, N. R. An analysis of chemical reactor stability and control. *Chem. Eng. Sci.* **1958**, *7*, 121−130.

(12) Uppal, A.; Ray, W. H.; Poore, A. B. On the Dynamic Behavior of Continuous Stirred Tank Reactors. *Chem. Eng. Sci.* **1974**, *29*, 967.

(13) Hyanek, I.; Zacca, J.; Teymour, F.; Ray, W. H. Dynamics and Stability of Polymerization Process Flow Sheets. *Ind. Eng. Chem. Res.* **1995**, *34*, 3872.

(14) Dangelmayr, G.; Stewart, I. Sequential Bifurcations in Continuous Stirred Tank Reactors Coupled in Series. *SIAM J. Appl. Math.* **1985**, *45*, 895.

(15) Kubicek, M.; Hofmann, H.; Hlavacek, V.; Sinkule, J. Multiplicity and Stability in a Sequence of Two Nonadiabatic Nonisothermal CSTRs. *Chem. Eng. Sci.* **1979**, *35*, 987.

(16) Varma, A. On the Number and Stability of Steady States of a Sequence of Continuous Stirred Tank Reactors. *Ind. Eng. Fundam.* **1980**, *19*, 316.

(17) Snovoros, S.; Aris, R.; Stephanopoulos, G. On the Behavior of Two Stirred Tanks in Series. *Chem. Eng. Sci.* **1982**, *37*, 357.

(18) Simon, R. H. M.; Chappelear, D. C. In *Polymerization Reactors and Processes*; Henderson, J. N., Bouton, T. C. Eds.; American Chemical Society: Washington, DC, 1976; Chapter 4.

(19) Varazaluce-García, J. C.; Flores-Tlacuahuac, A.; Saldívar-Guerra, E. Steady-state Nonlinear Bifurcation analysis of a High-Impact Polystyrene Continuous Stirred Tank Reactor. *Ind. Eng. Chem. Res.* **2000**, *39*, 1972.

(20) Dhooge, A.; Govaerts, W.; Kuznetsov, Y. MATCONT: A Matlab Package for Numerical Bifurcation Analysis of ODEs. *ACM Trans. Math. Software* **2003**, *29*, 141.

(21) Chen, C. Simulation of a Continuous Bulk Styrene Polymerization Process with Catalytic Initiation for Crystal-Clear

Polystyrene and Rubber-Modified Polystyrene. *Polym. React. Eng.* **1998**, *6*, 3−4.

(22) Estenoz, D. A.; Meira, G.; Gómez, N.; Oliva, H. M. Mathematical Model of a Continuous Industrial High-Impact Polystyrene Process. *AIChE J.* **1998**, *44*, 427−441.

(23) Flores-Tlacuahuac, A.; Saldívar-Guerra, E.; Ramírez-Manzanares, G. Grade Transition Dynamic Simulation of HIPS Polymerization Reactors. *Comput. Chem. Eng.*, submitted for publication.

(24) Hui, A. W.; Hamielec, A. E. Thermal polymerization of styrene at high conversions and temperatures. An experimental study. *J. Appl. Polym. Sci.* **1972**, *16* (3), 749−769.

(25) Villalobos, M. A.; Hamielec, A. E.; Wood, P. E. Kinetic Model for Short-Cycle Bulk Styrene Polymerization Through Bifunctional Initiators. *J. Appl. Polym. Sci.* **1991**, *40*, 1289.

(26) Peng, F. M. Polybutadiene Grafting and Cross-linking in High-Impact Polystyrene Bulk Thermal Process. *J. Appl. Polym. Sci.* **1990**, *40*, 1289.

(27) Fourer, R.; Gay, D. M.; Brian, W.; Kernighan, A. Modeling Language for Mathematical Programming. *Manage. Sci.* **1990**, *36*, 519.

(28) Wächter, A. W. Interior Point Methods for Large-Scale Nonlinear Programming with Applications in Process Systems Engineering, Ph.D. Thesis, Carnegie Mellon University, Pittsburgh, PA, 2002.

(29) Maciejowski, J. M. *Predictive Control with Constraints*; Prentice-Hall: 2002.

(30) Prasad, V.; Schenley, M.; Bequette, B. W. Product Property and Production Rate Control of Styrene Polymerization. *J. Process Control* **2002**, *12* (3), 353−372.

(31) Jensen, K. F.; Ray, W. H. The Bifurcation Behavior of Tubular Reactors. *AIChE J.* **1987**, *33*, 1300.

(32) Chavez, R.; Seader, J. D.; Wayburn, T. L. Multiple steady-state solutions for interlinked separation systems. *Ind. Eng. Chem. Fundam.* **1986**, *25* (4), 566−576.

(33) Russo, L. P.; Bequette, B. W. Operability of Chemical Reactors. Multiplicity Behavior of a Jacketed Styrene Polymerization Reactor. *Chem. Eng. Sci.* **1998**, *53* (1), 27−45.

(34) Kubicek, M.; Marek, M. *Computational Methods in Bifurcation Theory and Dissipative Structures*; Springer: New York, 1983.

(35) Sistu, P.; Bequette, B. W. Model Predictive Control of Processes with Input Multiplicities. *Chem. Eng. Sci.* **1995**, *50* (6), 921−936.

(36) Flores-Tlacuahuac, A.; Biegler, L. T.; Saldívar-Guerra, E. Optimal Grade Transitions in the HIPS Polymerization Process. Manuscript in preparation, 2004.

(37) Chen, L.-H.; Chang, H.-C. Global Effects of Controller Saturation on Closed-loop Dynamics. *Chem. Eng. Sci.* **1985**, *40*, 2191−2205.

(38) Cook, P. A. Simple Feeback Systems with Chaotic Behaviour. *Syst. Control Lett.* **1985**, *6*, 223−227.

(39) Alvarez, J.; Curiel, L. E. Bifurcations and Chaos in a Linear Control System with Saturated Input. *Int. J. Bifurcation Chaos* **1997**, *7* (8), 1811−1822.

(40) Russo, L. P.; Bequette, B. W. Bifurcation Analysis of Cascade Controlled Nonlinear Systems, 13th World Congress of IFAC, session 7a-11 (Chemical Process Control II), San Francisco, CA, June/July 1996.

Received for review July 2, 2004
Revised manuscript received December 23, 2004
Accepted January 3, 2005

IE049418M